

# Properties of Microcrystalline Cellulose and Powder Cellulose After Extrusion/Spheronization as Studied by Fourier Transform Raman Spectroscopy and Environmental Scanning Electron Microscopy

Submitted: March 25, 2003; Accepted: October 21, 2003; Published: November 19, 2003

Petra M. Fechner,<sup>1</sup> Siegfried Wartewig,<sup>2</sup> Manfred Fütting,<sup>3</sup> Andreas Heilmann,<sup>3</sup> Reinhard H.H. Neubert,<sup>1</sup> and Peter Kleinebudde<sup>4</sup>

<sup>1</sup>Institute of Pharmaceutics and Biopharmaceutics, Martin Luther University Halle-Wittenberg, Wolfgang-Langenbeck-Str. 4, 06120 Halle, Germany

<sup>2</sup>Institute of Applied Dermatopharmacy, Martin Luther University Halle-Wittenberg, Wolfgang-Langenbeck-Str. 4, 06120 Halle, Germany

<sup>3</sup>Fraunhofer Institute for Mechanics of Materials, Heideallee 19, 06120 Halle, Germany

<sup>4</sup>Institute of Pharmaceutical Technology, Heinrich Heine University Düsseldorf, Universitätsstr. 1, 40225 Düsseldorf, Germany

## ABSTRACT

In this study, the effect of powder cellulose (PC) and 2 types of microcrystalline cellulose (MCC 101 and MCC 301) on pellet properties produced by an extrusion/spheronization process was investigated. The different investigated types of cellulose displayed different behavior during the extrusion/spheronization process. Pure PC was unsuitable for extrusion, because too much water was required and the added water was partly squeezed during the extrusion process. In contrast, MCC 101 and MCC 301 were extrudable at a wide range of water content, but the quality of the resulting products varied. In the extrusion/spheronization process, MCC 101 was the best substance, with easy handling and acceptable product properties. The properties of the extrudates and pellets were determined by Fourier transform (FT) Raman spectroscopy and environmental scanning electron microscopy (ESEM). FT-Raman spectroscopy was able to distinguish between the original substances and also between the wet and dried extrudates. The particle sizes of the raw material and of the extrudates were determined by ESEM without additional preparation. For MCC, the size of the resulting particles within the extrudate or pellet was smaller. However, in the extrudates of PC, changes in particle size could not be observed.

**KEYWORDS:** powder cellulose, microcrystalline cellulose, pellet, Raman spectroscopy, environmental scanning electron microscopy, extrusion/spheronization

## INTRODUCTION

Cellulose derivatives are important pharmaceutical excipients. Usually, cellulose is produced from wood by washing, bleaching, purifying, and drying. Powder cellulose (PC) is generally obtained by mechanically micropulverizing cellulose. It has a high amount of amorphous regions and is often used as filler and binder in tablet manufacture. Microcrystalline cellulose (MCC) has a higher degree of crystallinity because it is usually obtained by partially hydrolyzing cellulose with mineral acid. Subsequently, porous raw material was achieved by spray-drying. MCC is mainly used as dry binder in manufacturing of tablets as well as in wet granulation, and it is the most important excipient in the extrusion process.<sup>1,2</sup>

Fourier transform (FT) Raman spectroscopy, a nondestructive method, yields information about the molecular structure of products. Some reports have compared Raman and infrared spectroscopy used for characterization of natural cellulose<sup>3</sup> and other celluloses.<sup>4</sup> These confirm the convenience of using Raman spectroscopy in similar studies. Raman spectroscopy needs only minimal sample preparation. In addition, water does not disturb measurement, which is a remarkable advantage. However, morphological information cannot be obtained.

**Corresponding Author:** Peter Kleinebudde, Institute of Pharmaceutics, Heinrich-Heine-University Düsseldorf, Universitätsstr. 1, 40225 Düsseldorf, Germany. Tel: +49 211 811 4220; Fax: +49 211 811 4251; Email: [kleinebudde@uni-duesseldorf.de](mailto:kleinebudde@uni-duesseldorf.de)

Conventional scanning electron microscopy (SEM) requires high vacuum conditions, and the nonconducting specimen surfaces need to be coated with a thin metal or carbon layer. In contrast, surfaces of untreated insulating materials can be investigated using environmental scanning electron microscopy (ESEM).<sup>5</sup> ESEM also allows for observation of the surface while wetting or drying. During such in situ investigations, the specimen can be kept in an equilibrium state with defined ambient humidity.

Different types of extruders are available to produce extrudates for further spheronization. The differences between a gravity-fed and a ram extruder have been considered in the literature. Baert et al,<sup>6</sup> using instrumented equipment capable to record important process variables like extrusion force, concluded that extrusion forces recorded with the ram extruder were always greater. Moreover, equivalent quality of spheres required greater water content when the ram extruder was used. Dietrich<sup>7</sup> described the instrumentation of a single screw extruder with axial discharge. He reported that an increase in screw rotation speed led to an increase in extrusion pressure but that the quality of the resulting pellets was not adversely affected. This observation appears contrary to that of Harrison et al,<sup>8</sup> who reported that low extrusion rates were recommended for improving the quality of pellets. After using a ram extruder, Harrison et al<sup>8</sup> reported that decreasing the ram speed could eliminate "shark skinning" of the extrudate, which can severely mar the quality of the product. They also point out that ram speed cannot increase toward these critical velocities when extrusion is through multiholed dies. In this study, a twin-screw extruder was used. In contrast to the single-screw extruder, which is always operated with a completely filled barrel, a twin-screw extruder is running in a "starved" modus, that is, with incomplete filling of the barrel. An increase in screw speed using a single-screw extruder results in a higher extrusion rate and thus a higher extrusion pressure, whereas in a twin-screw extruder the extrusion rate is constant but the pressure decreases because less material is in the extrusion barrel.<sup>9</sup>

Two models were suggested in the literature to explain the behavior of MCC during extrusion/spheronization, namely the sponge model by Fielden et al<sup>10</sup> and the crystallite-gel model by Kleinebudde.<sup>11</sup> In this context, the influence of the degree of polymerization of different cellulose types during extrusion/spheronization was analyzed<sup>12</sup> and the decreasing particle size after homogenization of MCC suspension was examined.<sup>13</sup> PC showed no remarkable particle size reduction. The wa-

ter repository of MCC as a spheronizing aid was discussed.<sup>14</sup> The content of MCC in formulations to produce pellets was investigated; the pellet formulation was influenced by the properties of other excipients.<sup>15-17</sup> Acceptable pellets containing PC instead of MCC were produced only by using a binder like sodium carboxymethylcellulose.<sup>18</sup> Saleh et al<sup>19</sup> already explored the production of PC and MCC pellets and compared their different pellet properties without looking at their molecular structure.

The objective of this study was to compare how the molecular and morphological properties of different cellulose types, PC and MCC, are influenced by the extrusion and spheronization process using the conjunction of ESEM and FT-Raman spectroscopy.

## MATERIALS AND METHODS

### Materials

MCC 101 (Avicel PH 101, FMC BioPolymer, Philadelphia, PA, and MCC Sanaq 101 G, Pharmatrans Sanaq AG, Basel, Switzerland), MCC 301 (Avicel PH 301, FMC BioPolymer), and PC (Elcema P 050, Degussa AG, Frankfurt/Main, Germany) were used as received. Demineralized water was used as a granulation liquid. Paracetamol (acetaminophen) was supplied by BASF AG (Ludwigshafen am Rhein, Germany).

### Methods

#### *Blending of Powders*

In some experiments, 5% paracetamol was added to the MCC for dissolution testing. Dry powders were mixed together at 25 rpm for 10 minutes in a lab blender (LM 20, L B Bohle Maschinen + Verfahren GmbH, Ennigerloh, Germany).

#### *Preparation of the Extrudates and Pellets*

The extrudates were prepared using a twin-screw extruder (Micro 27GL-28D, Leistritz, Nürnberg, Germany). The extruder had an axial discharge with 23 dies of 1 mm diameter and 2.5 mm length. Screw speed of 60 rpm and powder feed rate of 20 g/min were kept constant for MCC samples. For extrusion of PC, the screw speed was varied between 60 and 100 rpm at a powder feed rate of 20 g/min. By modifying the pump rate for the granulation liquid, we were able to find the suitable moisture level for production of nearly spherical pellets. For each batch, 500 g of the extruded mass was rounded in a spheronizer (RM-300, Schlüter

Maschinenfabrik GmbH & Co. KG, Neustadt am Rübenberge, Germany) with cross-hatched plate of 300 mm diameter at 1000 rpm for 5 minutes. The wet pellets were dried in a fluid-bed drier (Aeromatic ST 2EX, Aeromatic-Fielder AG, Bubendorf, Switzerland) at 60°C. The time of drying was  $2 \times 15$  minutes and  $2 \times 7$  minutes for the MCC 101 and MCC 301 pellets, respectively.

The water content of the extrudates (in percent) based on dry mass was determined gravimetrically after drying at 105°C for 24 hours.

#### *Shape and Size of the Extrudates and Pellets*

Thickness of the extrudates was characterized by mean diameter using light microscopy (stereo microscope SZX 9, Olympus, Tokyo, Japan). For each batch, 3 extrudates were measured (magnification  $\times 50$ ) at 10 points 200  $\mu\text{m}$  apart from each other. The pellet shape and size were determined by mean Feret diameter and aspect ratio of at least 1000 pellets of each sample using an image analysis program. Image analysis was conducted using a system consisting of a stereo microscope (SZX 9, Olympus), a ringlight with cold light source (Highlight 3001 with HL-VRL, Olympus), a digital camera (DIG1300C, Micromotion, Landshut, Germany), and a personal computer with data logging card and the software Image C (Imtronic, Berlin, Germany). For each batch, samples were obtained by using a rotary cone sample divider (Retschmühle PT, Retsch GmbH & Co KG, Haan, Germany). Images of the pellets at a suitable magnification were translated into binary images. Contacting pellets were separated by a software algorithm. If the separation failed, pellets were deleted manually. For each pellet, 36 Feret diameters were determined and used to calculate the mean Feret diameter. The ratio of the maximum Feret diameter and the Feret diameter perpendicular to the maximum Feret diameter is used as the aspect ratio. Statistical parameters for the sample were calculated after transfer to Excel 2000 (Microsoft, Unterschleißheim, Germany).

The size distribution of dried pellets was estimated by sieve analysis. Each sample was vibrated for 5 minutes by a Retsch Vibro using a series of 7 standard sieves (Retsch) in a range of 250 to 2000  $\mu\text{m}$ . From the size distribution, median and interquartile ranges were calculated. For each cellulose type, the pellet sample with the lowest aspect ratio combined with a small interquartile range was considered to have the best spherical pellets and the optimal moisture content for extrusion and spheronization in our experiments.

#### *Electron Microscopy*

ESEM investigations were carried out on untreated extrudates and pellets using an environmental scanning electron microscope (ESEM-E3, ElectroScan, Wilmington, MA) with an  $\text{LaB}_6$  cathode and an acceleration voltage of 10 to 20 kV. Through use of a water-cooled Peltier stage, the specimen was held at a constant temperature of 6°C. During evacuation, the specimen was kept wet by using an additional water reservoir. The ambient humidity was controlled by the applied water vapor low pressure inside the microscope. The drying process was followed over 3 steps. At first, extrudates were observed at 100% ambient humidity, which corresponded to a pressure of 7.0 Torr. Then the pressure was dropped down to 3.5 Torr, and the drying process was started. After 15 minutes of extrudate drying, an ambient humidity of 50% was reached and the samples were observed again. After 10 minutes of drying at a pressure of 2.1 Torr and an ambient humidity of 30%, the last observation step was realized. During this drying procedure, overview micrographs of the whole extrudate or pellet (magnification  $\times 50$  and  $\times 150$ ) and of surface structure at various points (magnification  $\times 500$ ) were taken.

In addition to the ESEM investigations, the dried samples were investigated by SEM (FEG-SEM S 4500, Hitachi, Japan, and JSM 6700F, JEOL, Japan) after surface coverage with an ultrathin (3 nm) carbenium film.

#### *FT-Raman Spectroscopy*

Raman spectra were recorded by a Bruker FT-Raman spectrometer RFS 100/S (Bruker Optik, Ettlingen, Germany) using a diode pumped Nd:YAG laser at an operating wavelength of 1064 nm. The measurements of the samples in glass tubes were performed at a 180° angle scattering geometry with 400 scans and a laser power of 350 mW at the sample location. The interferograms were apodized with the Blackman-Harris 4-term function and Fourier-transformed to give spectra with a resolution of 4  $\text{cm}^{-1}$ . The evaluation of the spectra was carried out using the Bruker OPUS software.

To compare the Raman spectra of all samples to each other, all spectra were normalized with respect to the carbon hydrogen (C-H) stretching band at 2894  $\text{cm}^{-1}$ .

#### *Dissolution Testing*

The paracetamol release from the pellets was studied using the rotating paddle method (USP 24, PTW II dissolution tester, PharmaTest Apparatebau GmbH, Hain-

burg, Germany). The 250 mg pellets from the optimal samples per batch of the 710 to 1000  $\mu\text{m}$  fraction were exposed to 900 mL of phosphate buffer set to pH 5.8 at a temperature of 37°C for 1 hour at 50 rpm ( $n = 5-6$ ). The samples were taken every 5 minutes. The released paracetamol was analyzed spectrophotometrically (Spectronic 601, Milton Roy Company, Ivyland, PA) at a wavelength of 243 nm.

## RESULTS

### *Behavior of PC and MCC During the Extrusion/Spheronization Process and the Properties of the Resulting Products*

The extrusion process depends on the substances used and the water content inside the extruder. When the water content inside the extruder was decreased, increased friction and particle resistance was observed. Also, the pressure at the die plate and the resulting shear forces increased.

The 3 examined cellulose types, PC, MCC 101, and MCC 301, showed different behaviors during extrusion/spheronization and different properties of their final products. PC was unsuitable for extrusion, because too much water was required and the added water was partly squeezed during the extrusion process as a result of the pressure inside the extruder. Although the pump rate for granulation liquid was adjusted for 399% water content, the resulting pellets contained only 187% and 208% at 60 rpm and at 100 rpm, respectively. After a short time, the extrusion process was terminated because water started squeezing out of the mass. Thus, just a small amount of extrudates was produced. These were relatively hard and stable, with an irregular surface. In contrast to PC, both types of MCC were easy to extrude within a wide range of water content. MCC 101 was extruded in a range of moisture level between 123% and 220% and MCC 301 between 95% and 127%. The moisture level for MCC 301 was crucial. If the moisture was too low, the extrudates became more fragile. With a higher moisture level, the extrudates became sticky and adhered to each other. In contrast to those of MCC 101, the extrudates of MCC 301 looked denser. Deep fissures were observed throughout the extrudates. The surface of the MCC 301 extrudates was smoother than that of the MCC 101 extrudates. In turn, these properties of MCC 301 extrudates affected the spheronization process. MCC 301 extrudates produced with a low water level resulted in oblong pellets, whereas agglomerated pellets (twins) were obtained with MCC 301 extrudates

produced with an excess amount of granulation liquid. The optimal moisture content with nearly spherical pellets was 112% (**Figure 1**). The basis of the estimation of optimal moisture content was the aspect ratio, that is the ratio of length and width of the pellets. Those ratios were measured and compared dependent on the water content of each batch of MCC type. In contrast, the pellets of MCC 101 displayed a nearly spherical shape within a wide range of moisture levels between 137% and 157%. As shown in **Table 1**, the optimal moisture was 147%. Therefore, MCC 101 is a better candidate for spheronization than MCC 301. Similar observations have been made by Koo and Heng,<sup>20</sup> who found that MCC grades of higher bulk density, eg MCC 301, required less water to produce pellets, and the pellets were of lower sphericity.

The addition of 5% paracetamol into the formulation reduced the required water amount. The optimal moisture levels for MCC 301 and MCC 101 decreased to 108% and to 135%, respectively.

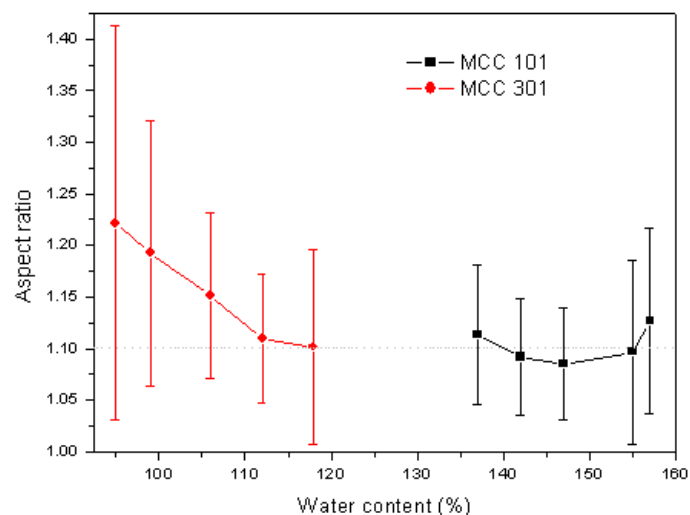


**Figure 1.** Aspect ratio of the pellets formed from MCC 101 and MCC 301 dependent on the extrudate water content.

The mean diameter of MCC and PC extrudates after drying supported in turn the observed behavior of the different cellulose types (**Figure 2**). Using the 1-mm-diameter dies, the mean diameter of the dried MCC extrudates decreased more than the mean diameter of the PC extrudates. For MCC, a higher water content during extrusion resulted in a smaller diameter of extrudates after drying.

**Table 1.** Data From Sieve Analysis ( $D_{gw}$ ,  $s_g$ ) and Image Analysis (Aspect Ratio, SD)\*

Sample	Water Content (%)	Median ( $\mu\text{m}$ )	IQR ( $\mu\text{m}$ )	Aspect Ratio	SD
MCC 101	137	917	270	1.114	0.067
	142	927	291	1.091	0.057
	147	913	252	1.085	0.054
	155	923	302	1.097	0.089
	157	1097	400	1.126	0.090
MCC 301	95	896	153	1.222	0.192
	99	938	305	1.193	0.129
	106	1015	354	1.151	0.081
	112	1122	305	1.100	0.063
	118	1173	237	1.102	0.095

\*IQR: Inter Quartile Range (D75-D25)

### Differences in the Morphological Structure of the Extrudates and Pellets

The ESEM investigations (**Figure 3**) showed that the extrudates of PC and MCC displayed different surface structures. Surfaces of PC extrudates were irregular, with deep and wide bulges. Electron microscopy results supported this observation as PC fibers showed no change in shape. Interestingly as seen in **Figure 3A**, they formed a porous network consisting of loosely packed particles with enclosed air bubbles.

Extrudates of MCC 301 and MCC 101 were more compact, but characteristic differences between the batches were observed (**Figure 3B-G**). Shape and size of extrudates depended on the MCC type and on the water content during the extrusion process. Surfaces of the extrudates of MCC 101 were uneven and showed more small fissures when the water content was increased. In contrast, surfaces of the extrudates formed from MCC 301 were smoother. No single particles could be identified. They seemed to be fused completely. However, fissures on the surface were seen throughout the whole extrudate and signed points of fractures. A view inside the extrudates and pellets showed different particle sizes and packages. Decreasing the amount of granulation liquid led to an increase in the shear forces during the extrusion. It was also obvious that the particle sizes within the MCC 101 extrudates became smaller when the water content was decreased (**Figure 3B-D**). This observation was related to the sample with the lowest water content, where the original cellulose fibers disappeared. As a result of the higher shear forces, only smaller fractures were found instead of original cellulose fibers. The same pattern was

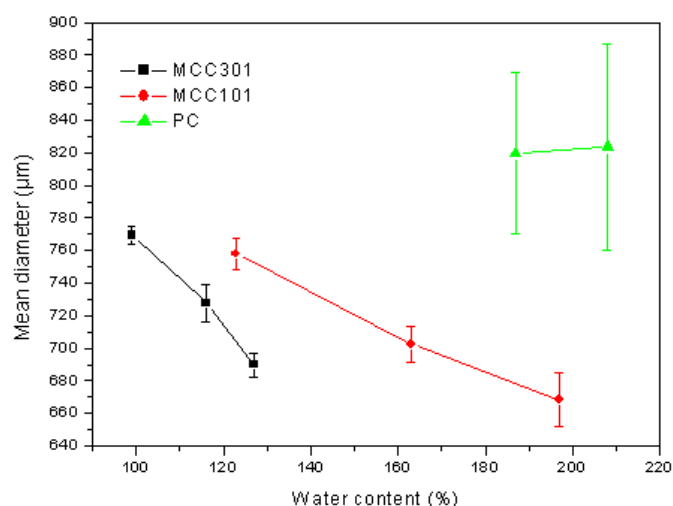


**Figure 2.** Mean diameter of extrudates formed from MCC and PC after oven-drying at 40°C.

observed in the micrographs of MCC 301 (**Figure 3E-G**).

**Figure 4** gives an overview of the surfaces of the resulting pellets produced with MCC 101 and 301. The pellets of MCC 101 were bigger than the MCC 301 pellets. Surfaces of whole pellets were smooth. **Figure 5** shows fractures and surfaces of MCC 101 pellets (**Figure 5A**) in comparison to MCC 301 pellets (**Figure 5B**) at higher magnification. It was clear that the surface of the pellets formed from MCC 101 was rougher than that of MCC 301 pellets. Additionally, pores were visible in fractures of pellets formed from MCC 101; these could not be found in the fractures of the extrudates. These pores might be a result of sample

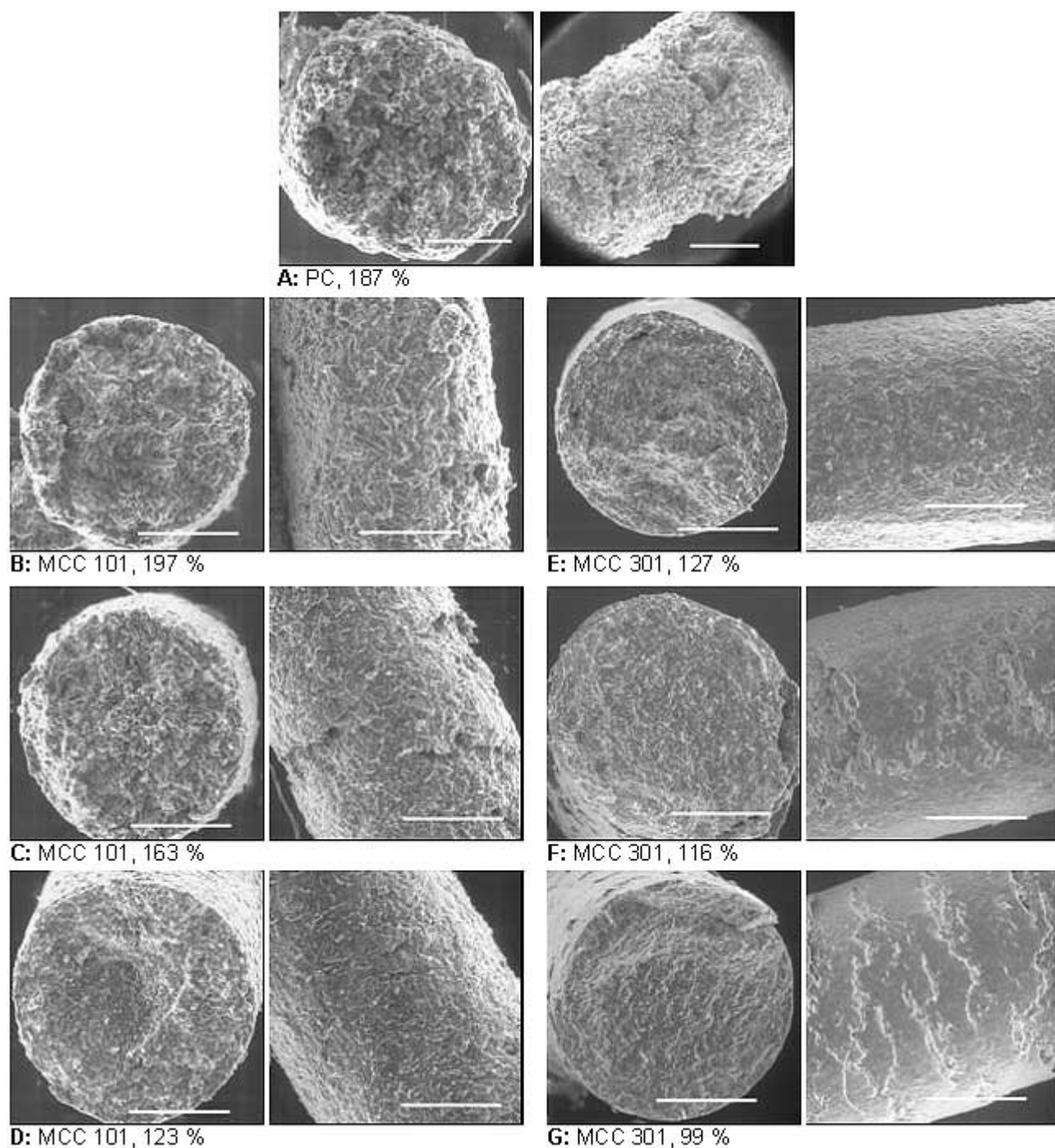


**Figure 3.** ESEM micrographs of fractures (left) and surfaces (right) of dried (40°C, 24 hours) extrudates of PC (A), MCC 101 (B-D), and MCC 301 (E-G) dependent on the extrudate water content (bar = 300  $\mu$ m). Pictures were taken without any additional coatings.

preparation. The pellets of MCC 301 showed no enclosed pores.

#### ***Behavior of Extrudates During the Drying Process***

The influence of the drying process on extrudate properties was investigated. Samples of extrudates of PC and MCC were dried for 24 hours at 40°C and at room temperature. Both procedures resulted in identical



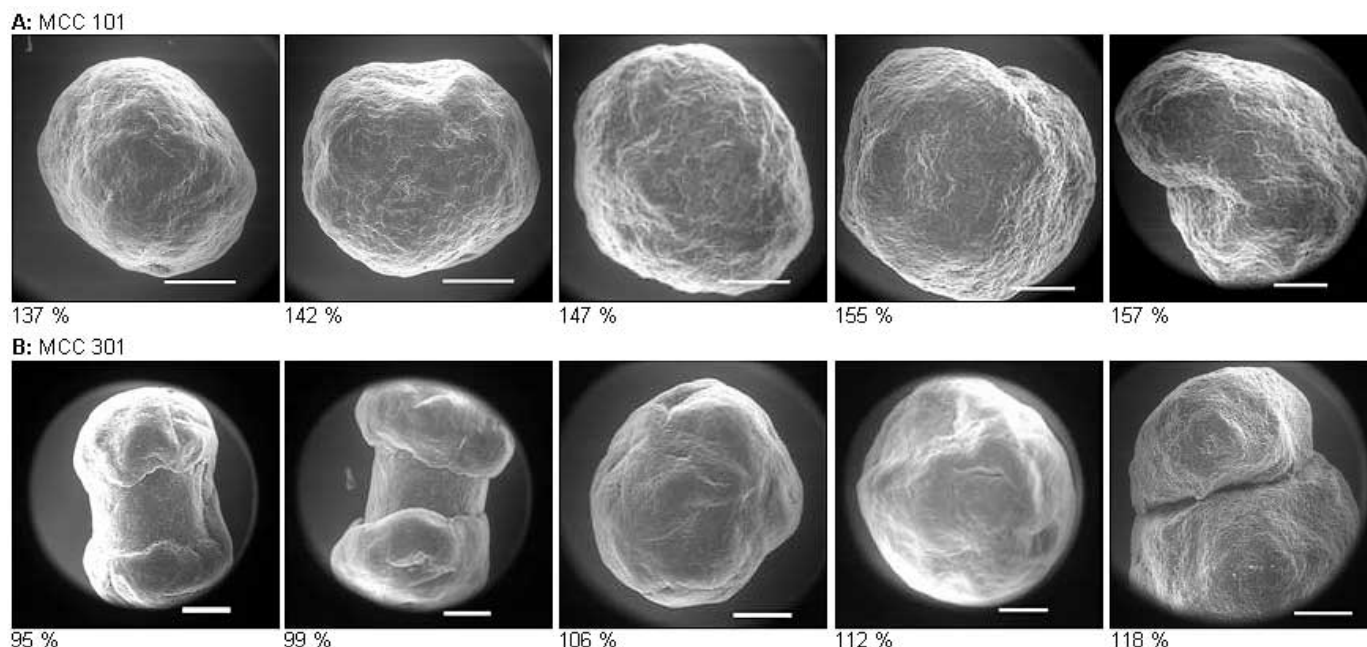


**Figure 4.** SEM micrographs of the dried pellet surfaces of MCC 101 (A) and MCC 301 (B) dependent on the extrudate water content (bar = 300  $\mu\text{m}$ ).

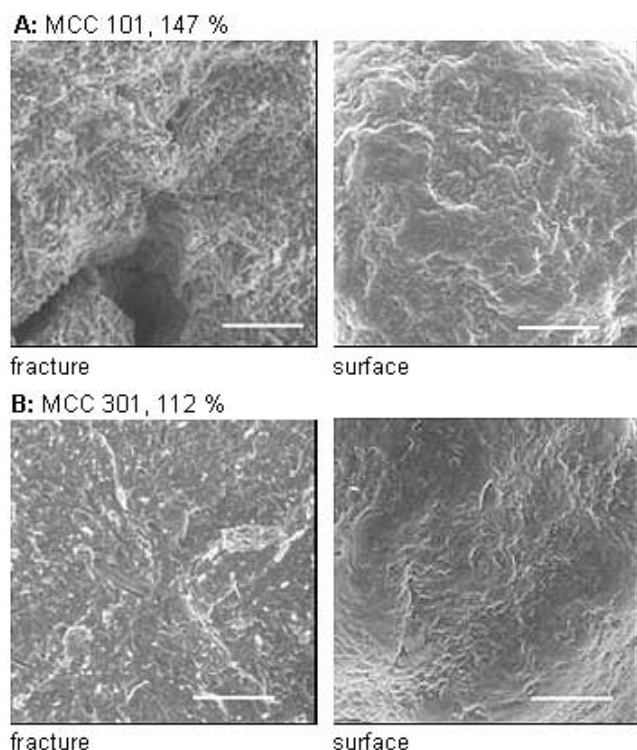


**Figure 5.** SEM micrographs of fractures and surfaces of dry pellets of MCC 101 (A) and MCC 301 (B) (bar = 100  $\mu\text{m}$ ).

products, as shown by ESEM, indicating no influence of the drying process on the properties of the products.

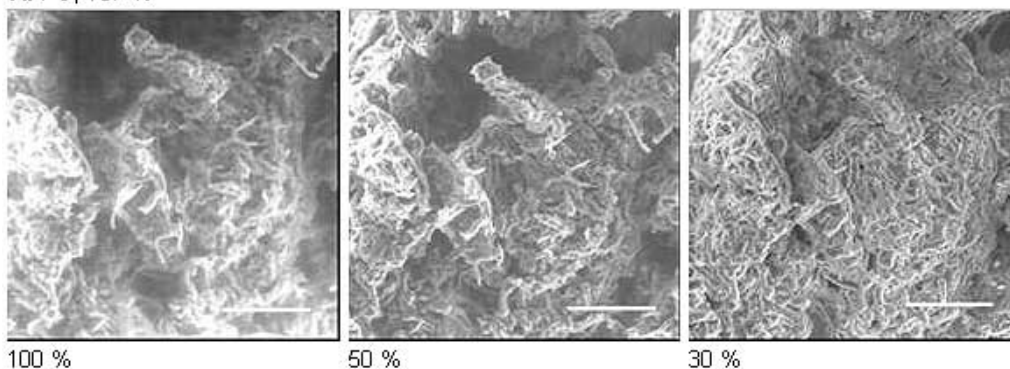
The morphological behavior of extrudates during drying was investigated by ESEM. Extrudates were dried in the ESEM under the applied low pressure. In most cases, cellulose fibers became smaller and the extrudate structures shrank together with decreasing relative humidity (**Figure 6**). However, it was not possible to quantify the extent of shrinking because similar structures behaved differently. Depending on their location, the extent of shrinking differed. In some cases, some structures even enlarged.

### Results of FT-Raman Spectroscopy

The Raman spectra of the raw material of PC and MCC are shown in **Figure 7**, where in each case the band in the C–H stretching region<sup>21</sup> between 2500 and 3100  $\text{cm}^{-1}$  is normalized. The Raman spectra of MCC 101 and MCC 301 clearly differ from those of PC. As expected, most bands of the PC spectra were broader than MCC bands because PC contains a higher amount of amorphous parts. Comparing the Raman spectra of PC with MCC, changes in the band intensities were found at 491, 519, 1095, 1120, 1265, and 1292  $\text{cm}^{-1}$  (see arrows in **Figure 7**).

The influence of water on the Raman spectra is shown in **Figure 8A** and **B**, where the spectra of MCC 101,

**A:** PC, 187 %



**B:** MCC 101, 123 %

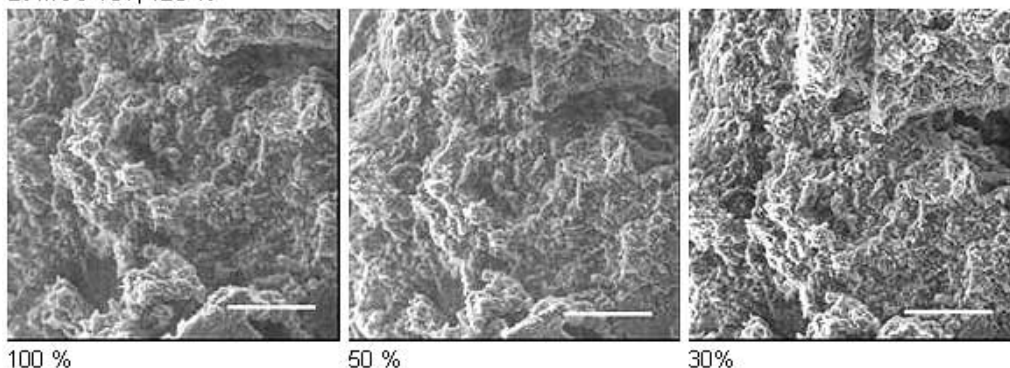


**Figure 6.** ESEM micrographs of extrudates of PC (187% extrudate water content) and MCC 101 (123% extrudate water content) during drying from 100% to 50% to 30% ambient humidity (bar = 100  $\mu\text{m}$ ).

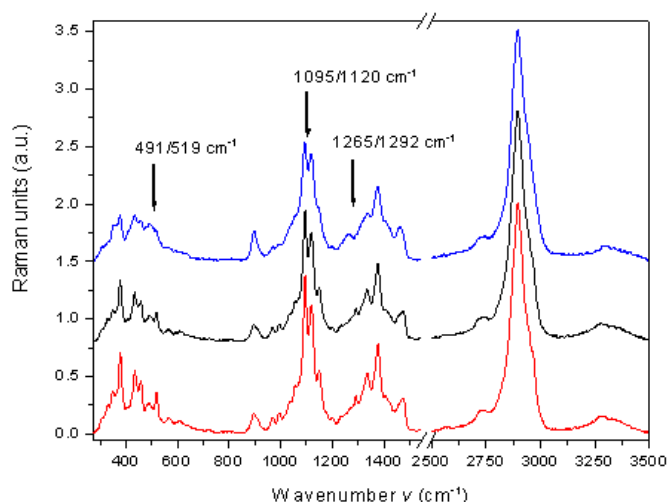


**Figure 7.** Raman spectra of the raw materials; from bottom to top: MCC 301, MCC 101, and PC. The spectra are normalized with respect to the C-H stretching band at 2894  $\text{cm}^{-1}$ . The arrows mark the differences between the spectra of the raw materials.

mixed with various amounts of water, together with the dry raw material are depicted. After water is added, a new shoulder appears at 2967  $\text{cm}^{-1}$  as a part of the C-H stretching mode between 2800 and 3000  $\text{cm}^{-1}$ . Broad O-H bands can be observed at 1640  $\text{cm}^{-1}$  and between 3100 and 3500  $\text{cm}^{-1}$ . With an increase amount of water, the O-H stretching vibration of the alcohol groups of glucose units with their maximum at 3274  $\text{cm}^{-1}$  changes to the O-H stretching mode of free water at 3230  $\text{cm}^{-1}$ , which is combined with a changing band shape, as shown in **Figure 8B**. The shift from 3274  $\text{cm}^{-1}$  to lower wavenumbers occurs at a moisture content between 55% and 73%. Furthermore, shifts in the peak positions of the O-H deformation at 1475  $\text{cm}^{-1}$  and of the C-O stretching ring mode at 1150  $\text{cm}^{-1}$  to higher wavenumbers follow from the interaction of the celluloses with water.

Differences in the Raman spectra of wet and dried extrudates were observed. Obviously, in the spectral range between 850 and 1800  $\text{cm}^{-1}$ , Raman bands of the wet extrudates exhibit a higher intensity than those of the dried samples, as shown in **Figure 9**. Of course, the broad Raman bands due to water at 1640 and 3230  $\text{cm}^{-1}$



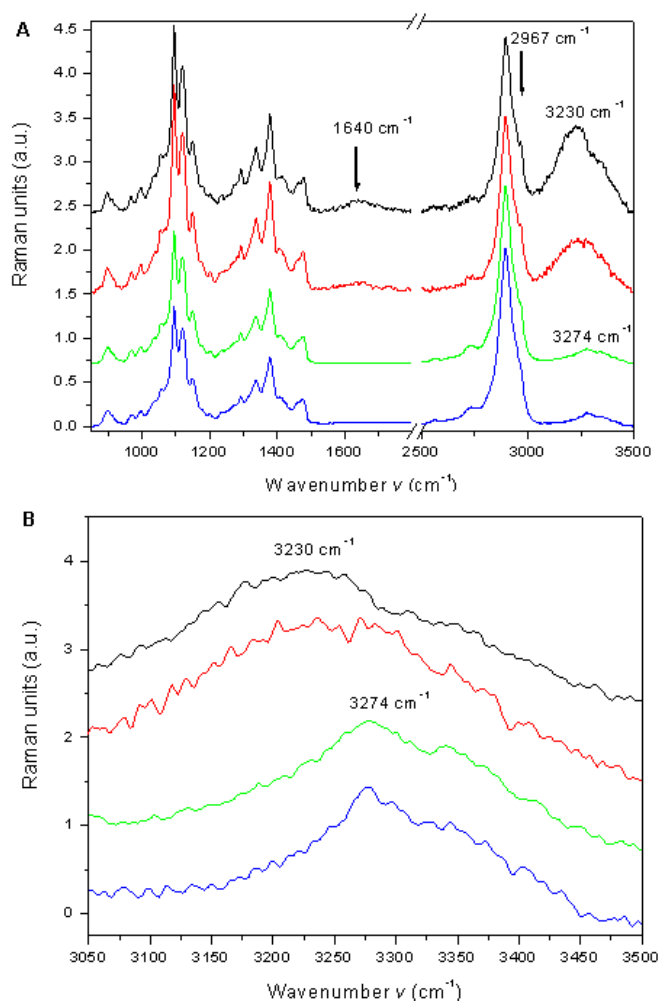


**Figure 8.** Raman spectra of the MCC 101 raw material compared with MCC 101 defined wet samples without extrusion exposition; from bottom to top: raw material and 17%, 123%, 267% water content. The spectra are normalized with respect to the C-H stretching band at 2894  $\text{cm}^{-1}$ . The arrows mark the changes due to the addition of water.

can be detected for the wet extrudate, too. On the other hand, the ESEM pictures do not give hints of any morphological changes due to drying in this case.

Both the ESEM pictures and the Raman spectra show that clear differences between dry and wet samples of MCC 101 were observed. The MCC 101 sample, extruded at 123% moisture, was exposed to the highest shear force during the extrusion and showed the strongest change in electron micrographs. As shown in **Figure 10**, for this sample, the Raman bands in the range between 850 and 1500  $\text{cm}^{-1}$  exhibit a lower intensity than those of the other wet extrudates. On the other hand, the Raman spectra of the MCC extrudates with 163%, 197%, and 220% moisture are almost iden-

tical and similar to those of the corresponding wet raw material. However, the wet sample of MCC 101 extruded with 123% water content shows a different behavior. First, the Raman bands at 1150 and 1475  $\text{cm}^{-1}$  that change position following the water influence described above were situated at lower wavenumbers than in the Raman spectra of the other wet extrudates. Second, the feature of the broad Raman band of the O-H stretching mode between 3100 and 3500  $\text{cm}^{-1}$  of the 123% product is different. The Raman band of the 163% and 197% products is represented at 3230  $\text{cm}^{-1}$  due to the O-H stretching mode of the free water. On the other hand, the 123% product shows the band at 3274  $\text{cm}^{-1}$  possible due to a transitional stage between the vibrations of OH groups of glucose units and free water. As shown in **Figure 11**, the Raman spectra of the MCC 101 raw material with 123% moisture and MCC 101 wet extrudates with 123% extrusion water content are clearly different. The Raman spectra of the extrudates show a lower intensity in the range between 850 and 1500  $\text{cm}^{-1}$  and another feature of the band between 3100 and 3500  $\text{cm}^{-1}$ . In spite of the acquired extrudate moisture of 123%, the spectra show more similarity to the spectra of MCC 101 raw material with 73% moisture. This finding hints that the extrusion with low water content could result in another interaction between water and cellulose.

### Dissolution Testing

**Figure 12** shows that only a minor difference in the drug dissolution between MCC 101 and MCC 301 was noticed. Both types of materials released paracetamol rapidly within a short time. After 15 minutes, 85% and 74% paracetamol were released from MCC 301 and MCC 101, respectively. However, at the end of the dissolution it was clear that MCC 301 released paracetamol slightly faster than MCC 101.

**Figures 13** and **14** show the pellets before and after dissolution. It was obvious that the MCC 301 pellets burst during dissolution. This could explain the unexpected rapid dissolution seen with MCC 301 pellets. Furthermore, on the MCC surface, pores were formed during dissolution testing. It is likely that the size of the pores is different for various MCC pellets. MCC 101 shows a higher amount of pores than MCC 301.

### DISCUSSION

Two models were suggested to describe the interaction between cellulose and water. Applying calorimetric studies on MCC, Fielden et al.<sup>10</sup> described MCC as a

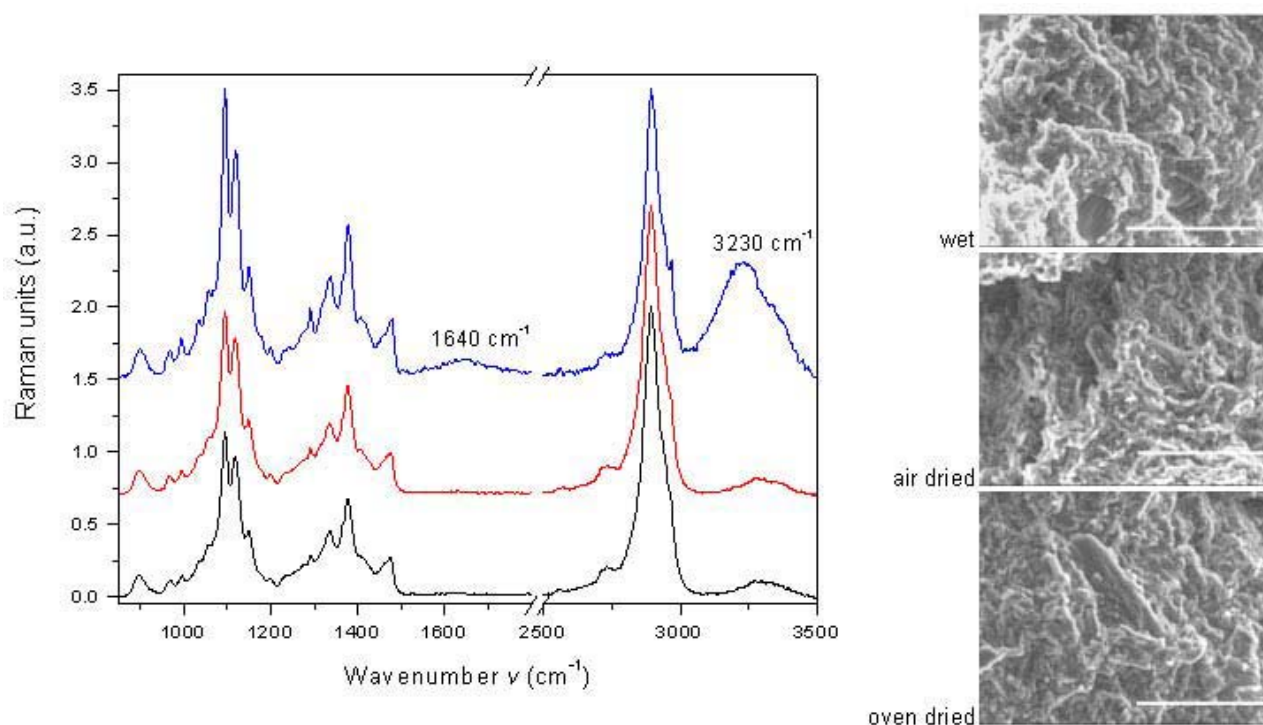


**Figure 9.** Raman spectra and ESEM micrographs of the extrudates formed from MCC 101 with 163% extrudate water content observed under wet conditions and air-dried as well as oven-dried ( $40^\circ\text{C}$ ) conditions; from bottom to top: oven-dried, air-dried, wet. The spectra are normalized with respect to the C-H stretching band at  $2894 \text{ cm}^{-1}$  (bar =  $100 \mu\text{m}$ ).

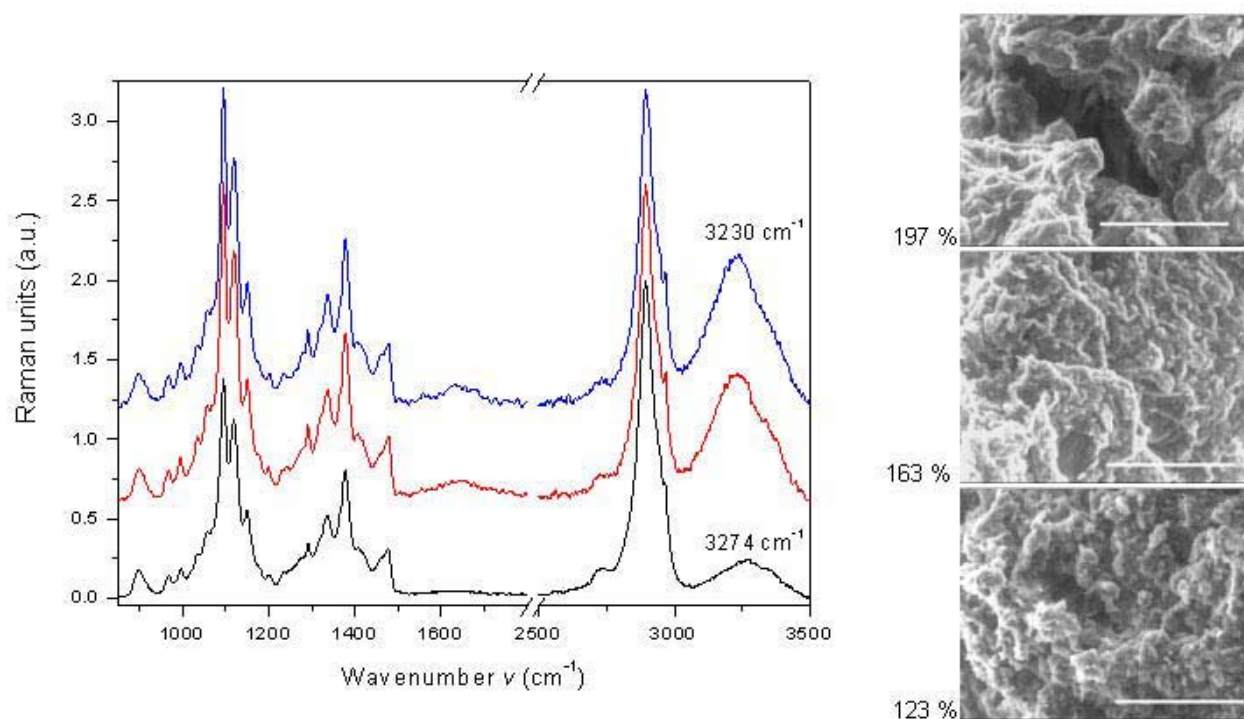


**Figure 10.** Raman spectra and ESEM micrographs of the wet extrudates of MCC 101 dependent on the extrudate water content; from bottom to top: 123%, 163%, 197%. The spectra are normalized with respect to the C-H stretching band at  $2894 \text{ cm}^{-1}$  (bar =  $100 \mu\text{m}$ ).

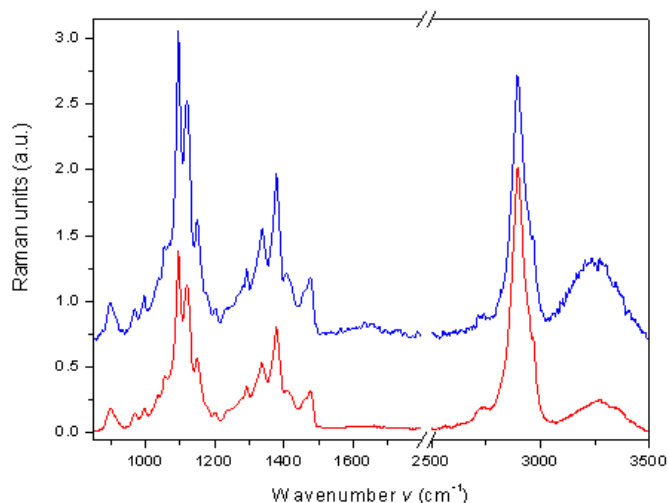


**Figure 11.** Raman spectra of the MCC 101 raw material with 123% water content (top) and of the MCC 101 wet extrudates with 123% extrudate water content (bottom). The spectra are normalized with respect to the C-H stretching band at  $2894\text{ cm}^{-1}$ .

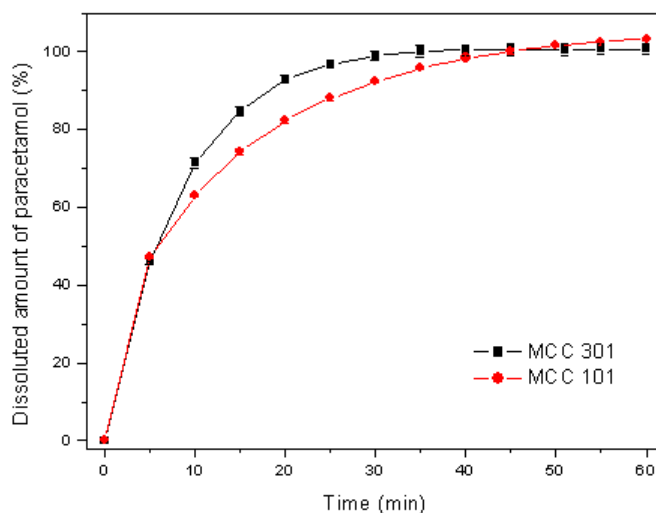


**Figure 12.** Dissolution of paracetamol from pellets with MCC 101 and MCC 301.

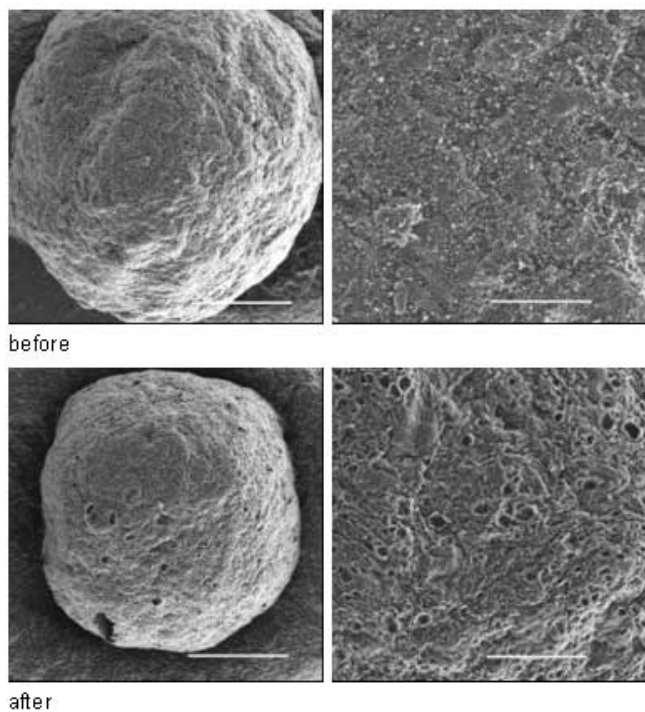


**Figure 13.** SEM micrographs of the pellets of MCC 101 before and after dissolution testing ( $\text{bar}_{\text{left}} = 300\text{ }\mu\text{m}$ ,  $\text{bar}_{\text{right}} = 60\text{ }\mu\text{m}$ ).

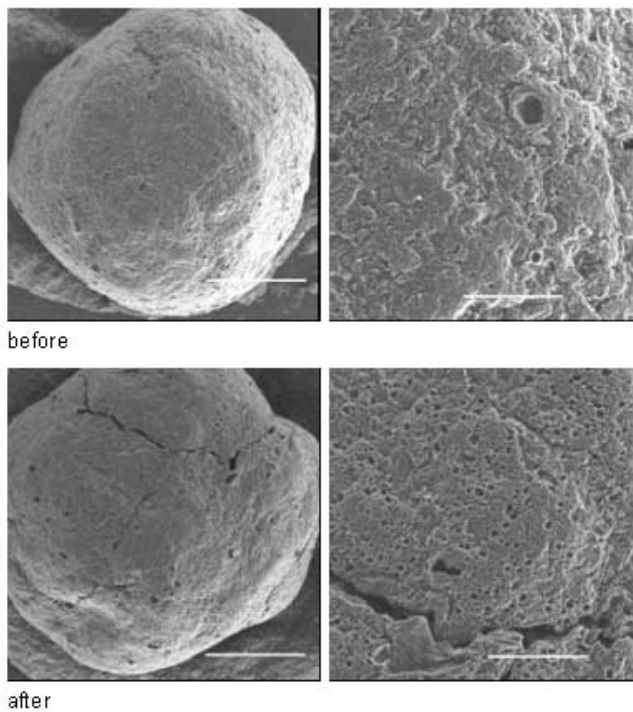


**Figure 14.** SEM micrographs of the pellets of MCC 301 before and after dissolution testing ( $\text{bar}_{\text{left}} = 300\text{ }\mu\text{m}$ ,  $\text{bar}_{\text{right}} = 60\text{ }\mu\text{m}$ ).

"molecular sponge" because of its ability to immobilize a high amount of water as free and adsorbed water. Kleinebudde<sup>11</sup> suggested the crystallite-gel model to explain the different properties of MCC as an extrusion/spheronization aid. In the presence of water and

pressure during extrusion, the original MCC particles break down into smaller particles, and partly into colloidal crystallites. These smaller particles are able to arrange again and form a finer network. The assignment of cellulose types to one of these models was said

to depend on the degree of polymerization.<sup>12</sup> Because PC exhibits a higher degree of polymerization value than MCC, it was supposed that PC shows a more spongelike behavior and MCC a more gel-like behavior.

The present experiments indicate that for an optimum extrusion process, a mixture of spongelike and gel-like behavior might be desirable. The results of our experiments show that a clear-cut distinction between sponge and crystallite-gel behavior is not possible. PC and MCC show different properties during the extrusion and spheronization process. While pure PC is unsuitable for extrusion, both MCC types are extruded simply. Differences in the behavior of MCC 101 and 301 appeared in the course of spheronization. MCC 101 produced nearly spherical pellets, whereas MCC 301 yielded twins and oblong pellets. In contrast to Saleh et al,<sup>19</sup> who were able to produce pellets formed from PC, we were unable to produce pellets with PC because water was squeezed under the pressure during extrusion. This behavior of PC and the interactions with water under the influence of pressure inside the extruder could be described as sponge-like. Such sponge-like material soaks up water, which will be immobilized as free water. Under pressure, the added water drops out from the system. Finally, the sponge returns to its initial shape.<sup>10</sup> The original cellulose fibers of PC extrudates can be identified using ESEM. In contrast, MCC shows a different behavior. Both types of MCC are able to take up water. During the extrusion process, water is retained in the mixtures. Increasing the shear force decreases the particle size of MCC extrudates. This behavior can be understood on the basis of the crystallite-gel model.<sup>11</sup>

Using FT-Raman spectroscopy, one can distinguish between PC and MCC. Furthermore, the influence of water on cellulose is evident in the spectra. Morphological changes due to extrusion can be correlated with changes in the Raman spectra.

With the ESEM technique, the surfaces of wet and dry PC and MCC were observed without additional surface preparation. These images, along with those from micrographs taken by conventional SEM, allowed us to observe differences in the surface morphologies of the pellets prepared at various extrusion parameters.

## ACKNOWLEDGEMENTS

The authors wish to thank the Deutsche Forschungsgemeinschaft for financial support (Ne 427/12-1 and He 2125/13-1).

## REFERENCES

- Wallace JW. Cellulose derivatives and natural products utilized in pharmaceuticals. In: Swarbrick J, Boylan JC, eds. *Encyclopedia of Pharmaceutical Technology*. New York, NY: Marcel Dekker; 1991;319-337.
- Newton JM. Extrusion and extruders. In: Swarbrick J, Boylan JC, eds. *Encyclopedia of Pharmaceutical Technology*. New York, NY: Marcel Dekker; 2002;1220-1236.
- Edwards HGM, Farwell DW, Williams AC. FT-Raman spectrum of cotton: a polymeric biomolecular analysis. *Spectrochim Acta A Mol Biomol Spectrosc*. 1994;50A(4):807-811.
- Langkilde FW, Svantesson A. Identification of celluloses with Fourier-Transform (FT) mid-infrared, FT-Raman and near-infrared spectrometry. *J Pharm Biomed Anal*. 1995;13(4/5):409-414.
- Hopfe J, Fütting M. Fundamentals and applications of environmental scanning electron microscopy. In: Wetzig K, Schulze D, eds. *In Situ Scanning Electron Microscopy in Materials Research*. Berlin, Germany: Akademie Verlag GmbH; 1995:219-240.
- Baert L, Remon JP, Knight P, Newton JM. A comparison between the extrusion forces and sphere quality of a gravity feed extruder and a ram extruder. *Int J Pharm*. 1992;86:187-192.
- Dietrich R. Food technology transfers to pellet production. *Manuf Chemist*. 1989;60:Aug:29-33.
- Harrison PJ, Newton JM, Rowe RC. Flow defects in wet powder mass extrusion. *J Pharm Pharmacol*. 1985;37:81-83.
- Kleinebudde P, Lindner H. Experiments with an instrumented twin-screw extruder using a single-step granulation/extrusion process. *Int J Pharm*. 1994;94:49-58.
- Fielden KE, Newton JM, O'Brien P, Rowe RC. Thermal studies on the interaction of water and microcrystalline cellulose. *J Pharm Pharmacol*. 1988;40:674-678.
- Kleinebudde P. The crystallite-gel-model for microcrystalline cellulose in wet-granulation, extrusion, and spheronization. *Pharm Res*. 1997;14(6):804-809.
- Kleinebudde P, Jumaa M, Saleh FE. Influence of degree of polymerization on behavior of cellulose during homogenization and extrusion/spheronization. *AAPS PharmSci*. 2000;2(2):article 21.
- Jumaa M, Saleh FE, Hassan I, Müller BW, Kleinebudde P. Influence of cellulose type on the properties of extruded pellets, I: physicochemical characterisation of the cellulose types after homogenisation. *Colloid Polym Sci*. 2000;278(7):597-607.
- Heng PWS, Koo OMY. A study of the effects of the physical characteristics of microcrystalline cellulose on performance in extrusion spheronization. *Pharm Res*. 2001;18(4):480-487.
- Kristensen J, Schaefer T, Kleinebudde P. Direct pelletization in a rotary processor controlled by torque measurements, II: effect of changes in the content of microcrystalline cellulose. *AAPS PharmSci*. 2000;2(3):article 24.
- MacRitchie KA, Newton JM, Rowe RC. The evaluation of the rheological properties of lactose/microcrystalline cellulose and

water mixtures by controlled stress rheometry and the relationship to the production of spherical pellets by extrusion/spheronization. *Eur J Pharm Sci.* 2002;17:43-50.

17. Law MFL, Deasy PB. Use of hydrophilic polymers with microcrystalline cellulose to improve extrusion-spheronization. *Eur J Pharm Biopharm.* 1998;45:57-65.

18. Lindner H, Kleinebudde P. Use of powdered cellulose for the production of pellets by extrusion/spheronization. *J Pharm Pharmacol.* 1994;46:2-7.

19. Saleh FE, Jumaa M, Hassan I, Kleinebudde P. Influence of cellulose type on the properties of extruded pellets, II: production and properties of pellets. *STP Pharm Sci.* 2000;10(5):379-385.

20. Koo OMY, Heng PWS. The influence of microcrystalline cellulose grade on shape and shape distributions of pellets produced by extrusion-spheronization. *Chem Pharm Bull.* 2001;49(11):1383-1387.

21. Blackwell J, Vasko PD, Koenig JL. Infrared and Raman spectra of the cellulose from the cell wall of *Valonia ventricosa*. *J Appl Phys.* 1970;41:4375-4379.